Magnetic Nanoparticles for Medical Applications: Updated Review

Guadalupe Gabriel Flores-Rojas [1,2,3,*], **Felipe López-Saucedo** [2], **Ricardo Vera-Graziano** [3], **Eduardo Mendizabal** [1] **and Emilio Bucio** [2,*]

1 Departamentos de Química e Ingeniería Química, Universidad de Guadalajara, Centro Universitario de Ciencias Exactas e Ingenierías, Blvd. M. García Barragán#1451, Guadalajara 44430, Mexico; cddciq@cucei.udg.mx

2 Departamento de Química de Radiaciones y Radioquímica, Instituto de Ciencias Nucleares, Universidad Nacional Autónoma de México, Circuito Exterior, Ciudad Universitaria, Mexico City 04510, Mexico; felipelopezsaucedo@gmail.com

3 Instituto de Investigaciones en Materiales, Universidad Nacional Autónoma de México, Circuito Exterior, Ciudad Universitaria, Mexico City 04510, Mexico; graziano@unam.mx

* Correspondence: ggabofo@hotmail.com (G.G.F.-R.); ebucio@nucleares.unam.mx (E.B.)

Abstract: Magnetic nanoparticles (MNPs) represent an advanced tool in the medical field because they can be modified according to biomedical approaches and guided by an external magnetic field in the human body. The first objective of this review is to exemplify some promising applications in the medical field, including smart drug-delivery systems, therapies against cancer cells, radiotherapy, improvements in diagnostics using magnetic resonance imaging (MRI), and tissue engineering. Complementarily, the second objective is to illustrate the mechanisms of action and theoretical foundations related to magnetoresponsive materials.

Keywords: magnetic drug delivery; hyperthermia; superparamagnetic; nanoparticles; superconductors

1. Introduction

Magnetic nanoparticles (MNPs) are nanoscale particles (1–100 nm) that can be guided through an external magnetic field due to their superparamagnetic, ferrimagnetic, and ferromagnetic properties, which may provide features for biomedical applications. MNPs with superparamagnetic properties are of special interest because they exhibit strong magnetic interactions under an external magnetic field, which disappear once the external magnetic field is removed. This property allows for the design of ferrofluids, since MNPs can be stabilized in solutions because they do not present magnetic interactions when the external magnetic field is switched off; and allows for in vivo performance, as in (i) cell marking [1], (ii) drug systems guided by a magnetic field [2], (iii) image contrast agents [3], and (iv) as heat generators in hyperthermia treatments [4].

MNPs generally contains two main parts: the core and the coating. The core presents a predominant quantum effect, which commonly incorporates magnetic elements such as Fe, Ni, or Co as well as their corresponding oxides, while the coating is responsible for stabilizing and protecting the core from the chemical effects of the medium [5]. The coating also plays an essential role since it provides specific properties and functions to the nucleus; for example, biocompatible natural polymers, such as chitosan or cellulose, work as cargo vectors of therapeutic agents to release in a controlled manner (Figure 1). Due to these characteristics, biomedical device synthesis has shown great interest in low toxic superparamagnetic MNPs, to avoid embolization or other secondary effects for the patient at the molecular or cellular level [6].
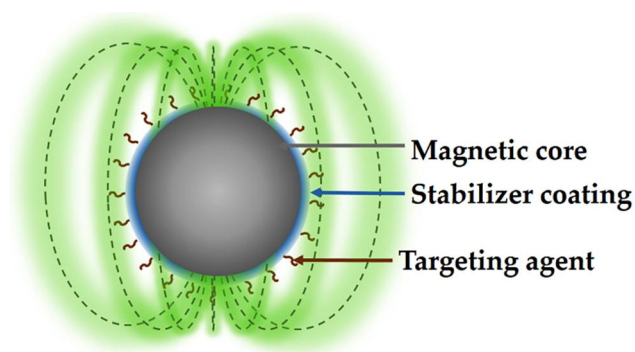
Figure 1. Structure of functionalized MNP for medical applications.

2. Synthesis of Magnetic Nanoparticles

The synthesis of nanoparticles (NPs) can be classified into three strategies: these are chemical, physical, and biological; chemical and physical classifications are widely used due to the significant number of synthesis methods that vary from precipitation to advanced methods and complex. Some of the most used synthesis methods are microemulsions [7], hydrothermal reactions [8], hydrolysis [9], sonolysis [10], thermolysis [11], electrochemistry [12], flow injection [13,14], electrospray [15], reduction [16], micellar [17], and gamma rays [18]; each of these methods are carried out in unique synthesis conditions that modify the physicochemical properties of MNPs, and therefore produce changes in their magnetic properties [19].

Precipitation and coprecipitation methods are widely used to obtain MNPs with a varied composition, such as Fe_3O_4 and $\gamma\text{-}Fe_2O_3$, as well as other NPs using a single element in their composition, such as Fe, Co, and Ni. However, some MNPs with medical applications have varied compositions, including metal and alloys such as Fe-Pd [20], Mn-Zn-Gd-ferrite [21], and lanthanides, for example, Ln(III):Fe_3O_4 (Sm, Eu, Gd) [22]. This methodology has also allowed for the synthesis of bioactive ferrimagnetic glass-ceramic MNPs with a layer of apatite similar to bone, which allow for the binding of proteins and drugs, providing adequate orientation to the affected tissue [23].

2.1. Precipitation and Coprecipitation

Precipitation and coprecipitation are easy and versatile methods that are widely used in the synthesis of MNPs with magnetic metal oxide nuclei from the corresponding salts in a basic medium, inert atmosphere, and at room or higher temperature, with the method being highly reproducible once the reaction conditions are adjusted, and therefore allowing for the size dispersion to be reduced [24]. This method's most common example of MNPs synthesized are Fe_3O_4 or $\gamma\text{-}Fe_2O_3$ NPs, obtained from Fe^{2+}/Fe^{3+}. The synthesis of this type of MNPs depends mainly on the sources of metal ions and factors such as temperature, pH, and ionic strength of the reaction medium. These MNPs presented low stability to environmental conditions, oxidizing or dissolving in the acid medium. Fe_3O_4 or $\gamma\text{-}Fe_2O_3$ MNPs can be oxidized as part of their synthesis by treating them with Fe^{3+} solution, resulting in stable MNPs in acidic and basic media.

However, despite the challenge of promoting uniform nucleation of the MNPs, the real task consists of controlling the particle size to obtain a narrow size distribution in a slow nuclei growth. One of the most important factors controlling nuclei growth is temperature since this can lead to the formation of a wide range of NP sizes since this synthesis method tends to produce quite polydisperse NPs. However, obtaining NPs with low dispersity is possible once the synthesis conditions are standardized and adequately controlled.

Currently, precipitation and coprecipitation methods include several additives in the NPs synthesis process, which have the main function of stabilizing them, and in addition, can act as a reducing agent promoting nucleation. Some compounds used as stabilizing or reducing agents are polyvinyl alcohol (PVA), poloxamers, poloxamines, oleic acid, and derivatives of poly(ethylene glycol) (PEG) or even liposomes [25]. For example, the

concentration of PVA and citric acid in the synthesis of MNPs can modify the size and shape of the NPs [26]. However, chelation of metal ions can affect nucleation, promoting the formation of larger particles due to the low availability of nuclei in the reaction system and resulting in a massive growth of the available nuclei, with the synthesis system being dominated by the particle growth. Moreover, the adsorption of additives on the nuclei as coatings can decrease the growth rate, favoring the formation of smaller NPs.

2.2. Thermal Decomposition

The synthesis of NPs by thermal decomposition consists of the heating decomposition of organometallic compounds in organic solvents (with a high boiling point) and in the presence of stabilizing agents (i.e., surfactants) [27,28]. Some of the organometallic precursors of NPs are, for example, those synthesized with acetylketonates, *N*-nitrosophenylhydroxylamine (cupferronates), carbonyls, among others having as metallic centers $Fe^{2+,3+}$, $Mn^{2+,3+}$, $Co^{2+,3+}$, $Ni^{2+,3+}$, and using fatty acids, oleic acids, and hexadecylamine as stabilizing agents are some examples [29]. The type of NPs that can be obtained will depend on the organometallic compound used as a source; for example, if the organometallic compound contains metallic centers with a zero-oxidation state (i.e., $Fe(CO)_5$), it will take place the formation of metallic NPs. On the other hand, organometallic compounds with cationic metal centers will form metal oxide NPs such as Fe_3O_4, from $[Fe(acac)_3]$ used as a precursor [30,31]. Furthermore, metal precursors can be combined in the reaction system, resulting in NPs with magnetic alloys such as $CoPt_3$ [32] and FePt [33]. These types of MNPs present a high anisotropy and magnetic susceptibility as well as large coercivities [34].

This synthesis method allows for the size and shape of the NPs to be controlled, mainly by the ratios of the reagents; that is, the source of metal ions, stabilizing agent, solvent, reaction time, and temperature, which modify the reaction rate, morphology, and size of the NPs. Another variable to consider is the type of stabilizer used. For example, the chain length of fatty acids as stabilizers modifies the reactivity of metal precursors; that is, by reducing the alkyl chain of fatty acids, the reaction rate increases. Some of these variables were used by Jana et al., who synthesized different types of metal oxide MNPs such as Fe_3O_4, Cr_2O_3, MnO, Co_3O_4, and NiO, controlling the size and shape through concentration and reactivity. For example, iron oxide MNPs were synthesized from metal fatty acid salts, obtaining almost monodispersed NPs with an adjustable size between 6–50 nm and shapes that included points and cubes with increasing reaction time [35].

On the other hand, water-soluble magnetite NPs were also synthesized using a straightforward synthesis consisting of $FeCl_3 \cdot 6H_2O$ as an iron source and 2-pyrrolidone as a coordination solvent [36]. The size of the NPs was controlled by the reaction time, giving the following sizes 4, 12, and 60 nm for the times of 1, 10, and 24 h, respectively. The reaction time also modified the morphology of the NPs, changing from spherical at an early stage to cubic over longer times. The same group recently developed a one-step synthesis of water-soluble MNPs using similar reaction conditions by adding a dicarboxyl-terminated PEG as a surface-protecting agent [37]. MNPs showed potential application as magnetic resonance imaging (MRI) contrast agents for diagnosing cancerous tissue.

Although metal oxide NPs are the most synthesized by thermal decomposition, it is also possible to obtain metal NPs using suitable metal carbonyl sources. The metallic NPs, in comparison with the NPs of their corresponding oxides, show a higher magnetization, being of particular interest not only in the medical area but also in the technological area, mainly in data storage. Some of the MNPs synthesized using carbonyl complexes are, for example, Fe MNPs, which were synthesized using $Fe(CO)_5$ as an iron source in the presence of polyisobutene in decalin under an inert nitrogen atmosphere at 170 °C [38], giving a particle size range of 2–10 nm and a polydispersity of 10%, depending on the $Fe(CO)_5$/polyisobutene ratio. In the case of cobalt MNPs, $[Co_2(CO)_8]$ was used as the cobalt source in the presence of aluminum alkyl compounds (AlR_3); the Co MNPs ranged from 3–11 nm by controlling the size of the alkyl (R) chain length. In addition, these particles showed strong oxidation under air atmosphere, requiring a subsequent treatment

to inhibit oxidation; such treatments were coatings with polymers, resulting in stable MNPs in air, being more attractive due to their easy handling, storage, and applications in oxidizing media.

2.3. Microemulsion

Microemulsions are produced by dispersing one immiscible liquid in another (commonly water), forming droplets between 1 and 50 nm, which are stabilized by a surfactant [39]. Microemulsions are used as a nanoreactor capable of forming NPs due to the formation of microdroplets that contain the desired reagents. These droplets collide and merge in the reaction system, mixing the reagents and carrying out the formation of NPs. However, this method's drawbacks are polydispersity, low yield of NPs, large volumes of solvents required, and poor versatility in metal precursors compared to coprecipitation and thermal decomposition synthesis methods. Therefore, microemulsion would be a complicated method of synthesizing NPs.

Despite the drawbacks of the microemulsion method, various NPs have been synthesized, such as Fe_3O_4 NPs or MFe_2O_4 alloys with Co, Cu, Ni, Cd, etc., modifying their magnetic properties by incorporating these elements. For example, $MnFe_2O_4$-type alloyed NPs with sizes between 4–15 nm were synthesized by reverse micelles using sodium dodecylbenzenesulfonate as a surfactant [40], and the results showed that the size of the MNPs was related to the ratio between the water and solvent. Similarly, Fe_3O_4 nanorods were synthesized using reverse micelles as sol–gel method and $FeCl_3 \cdot 6H_2O$ as metal source. The studies in the synthesis showed that the phase of nanorods can be controlled through the reaction conditions such as temperature, atmosphere, and hydration degree of the gels. On the other hand, MNPs alloyed with $CoFe_2O_4$ were obtained by mixing $FeCl_3$ and $Co(AcO)_2$, in the presence of sodium dodecyl sulfate. The size of the MNPs was controlled by the concentrations of the metal sources and the surfactant. The average size of the MNPs varied from 2 to 5 nm, with a high polydispersity from 30 to 35% [41].

2.4. Coatings of MNPs

In the last decade, the synthesis of MNPs has made significant progress [42]; however, some problems remain, such as maintaining the stability of the NPs for long periods of storage, since uncoated MNPs are not stable in aqueous media, forming aggregates that later precipitate, a behavior that has also been studied in blood. In addition, once the MNPs enter the body they begin to be absorbed by proteins to finally be phagocytosed by macrophages [43]. Therefore, one approach to overcome these drawbacks in MNPs is a necessary coating to eliminate or minimize their aggregation in a physiological environment and phagocytosis, which can be generated in situ or as a post-synthesis [44,45].

Amphiphilic polymers are generally used to coat the surface of MNPs; some examples are poloxamers, poloxamines, and PEG derivatives or even liposomes, which have also given encouraging results in the assemble of magnetoliposomes [25]. One of the most widely used polymers as coatings is PEG, which produces biocompatible coatings that confer several other properties to NPs, such as high stability and dispersion in aqueous solutions and a prolonged circulation time in the blood. On the other hand, the adequate functionalization of PEG chains can allow bioconjugation with different ligands or therapeutic agents, expanding its possible applications in the biomedical area [46–48]. However, one of the drawbacks of the coatings is the modification of the final diameter of the MNPs and their thickness, which can significantly affect the relaxation and distribution capacity in vivo [49]. Consequently, it is critical to provide NPs with an amphiphilic polymer coating of appropriate molecular weight and ratio when designing MNP-bearing probes for imaging and targeted therapy.

Despite significant advances in developing MNPs, some obstacles remain, mainly in developing coatings that can stabilize MNPs and provide a chemically functional surface for bioconjugation with "probe" ligands. In addition, several of the ligands and polymers used to stabilize MNPs show weak interactions, allowing for their easy separation under

physiological and storage conditions (Table 1). On the other hand, the degree of success of the MNPs depends mainly on the magnetic properties of the MNPs, which are entirely linked to their morphology, structure, and crystal uniformity, as well as the orientation of the MNPs given by conjugation with biomolecules. Another factor to consider is the size distribution, being preferable to a size less than 100 nm, allowing for the decrease in phagocytosis [50,51].

Table 1. Coatings of NPs with possible medical applications.

Coating	Advantages	Medical Application
PEG [52,53]	Enhanced water solubility, reduced phagocytosis, and increased blood circulation time	MRI, tumor diagnosis, and treatment
Polyethylenimine [54–56]	Good biocompatibility	Gene and vectors
PVA [57–59]	Elevated stability, reducing the particle aggregation	MRI, vectors, and bioseparation
Glucan [60–64]	Excellent stability and extended blood circulation time	Vectors, MRI
Liposome [65–68]	Good biocompatibility	Tumor treatment, thermotherapy, and MRI
Chitosan [69–71]	Good biocompatibility, essential small-molecule vitamin for the human body	Vector, thermotherapy, and radiotherapy
White blood cells [72,73]	Biomimetic properties, excellent biocompatibility	Vector, nanovaccines, and treatment

3. Magnetic Drug-Delivery System (MDDS)

Currently, the conventional way of administering drugs to patients is partially inefficient because only part of the drug reaches the site of interest. Therefore, the conventional ways of consuming drugs may be ineffective and even harm the human body caused by their poor selectivity to the diseased area. The benefit of MNPs combined with superconductors is their application in magnetic drug-delivery systems (MDDS), which have effectively transported and delivered drugs with greater precision in the required area. In general terms, the development and research of MDDS began in the 1970s, when there was a need for magnets capable of generating an appropriate magnetic field to systematically guide drug-loaded superparamagnetic NPs to a specific region to treat or give therapy to a disease. Recently, MDDS has become a fundamental method of therapy that uses a superconducting magnet with a magnetic field capable of guiding MNPs to a specific organ or tissue and subsequently administering a drug with a high concentration, allowing the high levels to be eradicated or reduce toxicity within normal tissue, providing promising advances in drug-delivery systems (DDS) [74]. Therefore, the need for drug vectors with superparamagnetic properties at the nanometric level has become essential for carrying out these treatments.

Another essential characteristic of MNPs, in addition to the magnetic properties of the nucleus, is the chemical functionalization of the surface, binding molecules of biological interest on their surface and allowing them to interact with cellular and subcellular structures, as well as with molecules, helping to increase their selectivity with sick tissues [75]. In this sense, MDDS can have various potential applications, highlighting the treatment of cancerous tissues because the drug is concentrated only in the affected tissue, increasing its efficacy and minimizing its side effects. The first clinical tests in treatments against cancer cells using MDDS showed effective results when tested in the affected areas [76].

The MDDS process initially involves introducing the MNPs into the bloodstream and then directed to the affected area through an external magnetic field, for finally concentrate the MNPs near to a magnet placed on the body surface. In this process, the blood flow

plays a fundamental role since it distributes the MNPs throughout the body and then concentrates them using a magnetic field, as shown in Figure 2 [77]. Therefore, MNPs must meet a specific size to reach diseased tissue because they must pass through the pulmonary capillaries and avoid phagocytosis. It is recommended that the MNPs have a size of less than 100 nm to achieve this goal, reducing pain in the surrounding tissue when concentrated. However, if the MNPs are too small, they will not be able to show the proper magnetic behavior to be directed adequately with an external magnetic field [78]. Ideally, MNPs should present a high magnetization at body temperature, and once the magnetic field is removed, they should not retain the magnetization, avoiding the formation of aggregates capable of forming emboli and facilitating their elimination from the body.
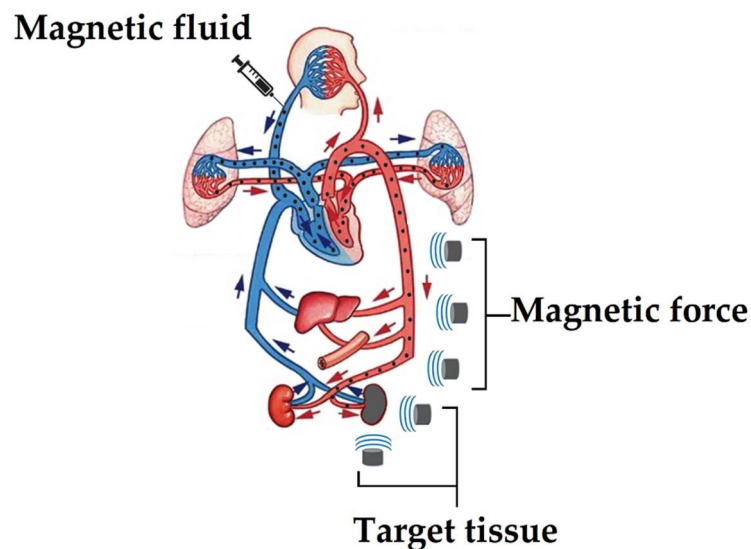

Figure 2. Pathway for a drug to reach a diseased part using MDDS.

One of the main challenges of external magnets applied in targeted drugs is their limited or relative application to superficial body targets, since deeply located tissues are difficult to treat because the magnetic force is reduced with distance, decreasing its effectiveness in manipulating and accumulating the MNPs conjugated with therapeutic agents [79]. Unfortunately, magnetic fields from large magnets used in internal tissue do not solve the problem as they present a low-gradient magnetic field, which reduces the retention capacity of MNPs [80]. Furthermore, since the magnetic force of magnets is proportional to the product of the gradient of their magnetic field, strong magnetic fields with a wide gradient are needed to overcome the hydrodynamic drag force produced by the bloodstream; otherwise, a build-up will occur with a limited number of MNPs as has been shown with some Halbach arrays, which have only been able to trap some magnetic microbubbles [81].

For this reason, the scientific community has devoted significant efforts to developing superconducting magnets that provide better results in the accumulation of MNPs in internal tissues; since the MNPs have a size of less than 100 nm, they have a markedly decreased magnetic susceptibility [82]. As a result, superconducting magnets capable of producing strong magnetic fields are needed to control MNPs from outside the body. In particular, bulk superconducting magnets are the most desirable for solving MNPs addressing problems in MDDS [83]. In this way, several researchers have designed new MDDS strategies using rotating magnetic fields in the desired area with high-temperature superconducting (HTS) magnets (magnets that work at temperatures above 77 K), allowing for an adequate accumulation of MNPs in deep tissue without invading other parts of the body.

Using permanent magnets or electromagnets to direct MNPs from an initial position to the desired tissue area is widely used [84]. However, permanent magnets have some dis-

advantages despite not requiring a power supply since it is difficult to adjust the magnetic field, unlike an electromagnet, which allows its magnetic field to be controlled through the operating current. Unfortunately, electromagnets can only generate a limited magnetic field, presenting complex handling due to their large sizes with low heat dispersion capacity (i.e., NbTi and Nb_3Sn coils), making them unsuitable for most cases of MDDS applications.

On the other hand, permanent magnets have been successfully exploited in MDDS [83], and HTS-type superconducting magnets are currently being tested, as is the case of Gd-Ba-Cu-O superconducting magnets capable of generating a 4.5 T magnetic field. These Gd-Ba-Cu-O magnets were used to direct magnetoliposomes as drug carriers through tap water and pig blood by placing the magnet at 50 mm and 25 mm, respectively, achieving excellent navigation in both cases and suggesting that the systems can be effective in vivo applications [85,86].

Likewise, a C_{60}-based solid could produce a strong magnetic field at low temperatures, 17 T at 29 K [87]; similarly, Gd-Ba-Cu-O, 3 T at 77 K [86]. For example, SmBaCuO and YBaCuO-type HTS were used as external magnetic field sources to drive 100 nm MNPs through a Y-shaped glass tube with blood flow. The results indicated a 90% accumulation of the NPs due to the magnetic force of the superconducting magnet at 20 mm (Figure 3). These experimental results indicate that MNPs can target and accumulate in a controlled manner, even at a flow rate of 100 mms^{-1} [88].
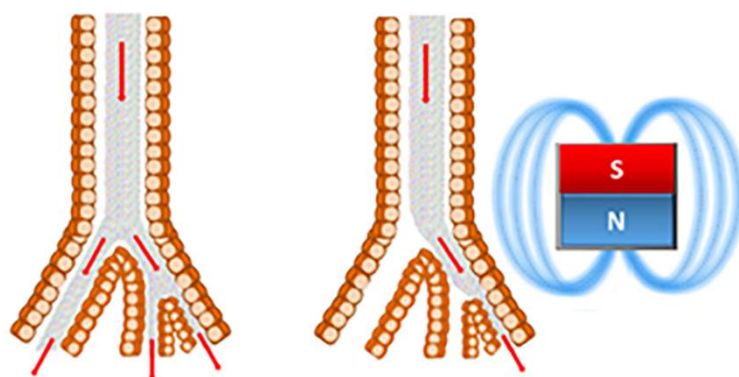

Figure 3. Schematic representation of an MDDS operated under the influence of external magnetic field.

4. Magnetic Hyperthermia

The concept of hyperthermia refers to an increase in temperature inside the body [89]. A classic treatment approach based on hyperthermia involves subjecting the patient to a local or total temperature increase in a range of 44–47 °C, a temperature considered optimal in cancer therapy.

In this sense, the process of thermoablation of cancer cells can be achieved through a discharge of electromagnetic waves generated by an electrode implanted in the pathological area at a radio frequency of between 0.1 and 1 MHz, thus activating various mechanisms of cell degradation and causing the death of cancer cells [90]. A less invasive system involves a series of external resonant microdevices that transfer energy to the tissues through radiation with light or electromagnetic waves and lasers. Various advanced techniques such as ultrasound, radiofrequency, or microwaves are currently being used to treat hyperthermia [91]. However, they may have some disadvantages, such as damage to healthy tissue surrounding cancer cells, limited heat infiltration into cancer tissue, and insufficient heat to treat some types of cancer tissue. Fortunately, all these limitations can be overcome by magnetic hyperthermia, which consists of MNPs in cancerous tissue and an external magnetic field with a high frequency, where the MNPs generate heat through the oscillation of their magnetic pulse [92].

Hyperthermia treatments can be classified into three types:

- **Local hyperthermia**: consists of an increase in temperature in a specific area of the tissue.

- **Regional hyperthermia:** an increased temperature is applied over large tissue areas, such as an organ or limb.
- **Whole-body hyperthermia:** is mainly used to treat pathogenic tissue spread throughout the body, such as metastatic cancer.

Among all types of hyperthermia, the most complicated to perform is local or regional hyperthermia due to the area of tissue that requires treatment. In this sense, magnetic hyperthermia offers a better solution for the selective treatment of cancer cells since the MNPs can be guided by an external magnetic field towards the cancerous tissue and subsequently initiate hyperthermia therapy employing magnetic pulses, thus reducing the doses of other treatments such as chemotherapy and radiotherapy [93].

The increase in temperature of MNPs is mainly due to the conversion of magnetic energy, determined by the specific absorption rate (SAR), which is defined as the rate of electromagnetic energy absorbed by biological tissue. The SAR depends on the amplitude, magnetic field frequency, and magnetic relaxation mechanisms of the MNPs, which depend on their morphology, size, and intrinsic magnetic parameters. With this technique, localized heat can be generated, reaching temperatures between 42 and 45 °C, a temperature at which it is possible to destroy cancer cells without causing damage to normal cells. Therefore, a significant challenge in hyperthermia therapy using MNPs is to ensure that their heating is properly controlled when transferred to the biological environment. However, this specificity is only achieved as long as specific targeting is achieved through the biofunctionalization of MNPs with molecules (i.e., coupling to antibodies) that direct them to the target of cancer cells [94,95].

Néel and Brownian relaxation are the main phenomena responsible for heating the MNPs. The Néel relaxation is determined by the rotation time of the magnetic moment and the return time to the equilibrium magnetization of the MNPs [96]. The magnification of the easy axes of the MNPs is blocked under conditions of high anisotropy, favoring a lower-magnetic-energy direction. Therefore, the Néel relaxation is defined as the fluctuation from the magnetic jumps from the easy axes (Figure 4). On the other hand, Brownian relaxation is based on the physical rotation of MNPs and their rotation from magnetic viscosity [97]. Figure 5 shows the magnetic relaxation components of a MNP capable of dissipating heat [98]. However, the relative heat contributions have not yet been evaluated, and since Brownian relaxation heat dissipation depends on the local environment, magnetic particles that dissipate heat by Néel relaxation [2], are preferred in clinical trials. This principle has been applied in suspensions of MNPs that have been used to treat patients with prostate and brain cancer with promising results [99].
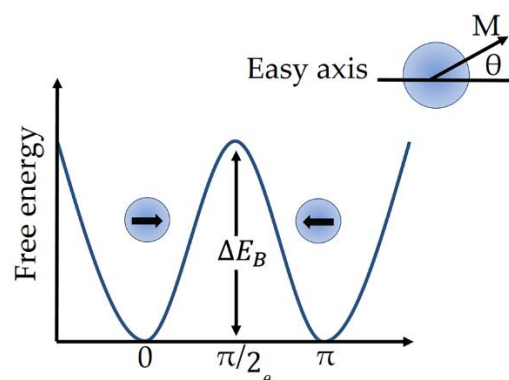

Figure 4. Evolution of the magnetic energy with the tilt angle between the easy axes.
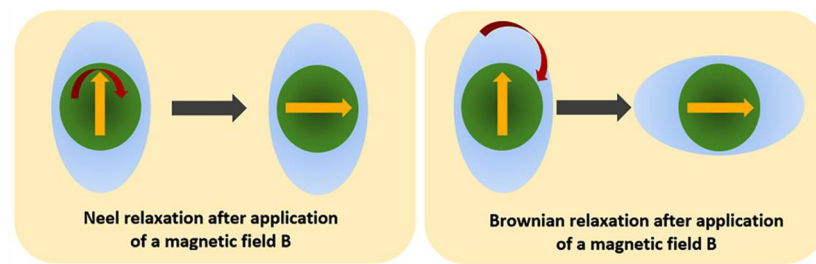
Figure 5. Néel relaxation is the rotation of magnetic moment inside a stationary MNP. Brownian relaxation is the rotation of entire MNP along with the magnetic moment.

Various research studies on the mechanism of heat generation have shown that the size of MNPs strongly affects the rate of heating [98]. Furthermore, due to the Brownian and Néel relaxation, time constants are modified depending on the particle. However, the SAR is the main parameter to determine the tissue heating rate. In general, the SAR is expressed in units of watts per kilogram (W/kg) and is proportional to the rate of temperature rise ($\Delta T/\Delta t$) for the adiabatic case, as shown by the following equation (Equation (1)):

$$SAR = 4.1868\frac{P}{m_e} = C_e\frac{dT}{dt} \tag{1}$$

where P is the electromagnetic wave energy absorbed by the sample, m_e is the mass of the sample, and C_e is the specific heat capacity of the sample.

The SAR can be affected by the electrical properties of the tissue, such as electrical permeability and conductivity, as it is when performing hyperthermia therapy with external magnetic antennas with a high irradiation frequency, which causes the formation of hot spots when carrying performed regional hyperthermia therapy [100]. Therefore, to avoid such phenomena, it is necessary to first dope the tissue with a ferrofluid followed by low-frequency irradiation (100–400 kHz).

SAR variability is also influenced by the nature of the MNPs and the volume ratio of particles in the tissue, with greater efficiency being achieved when the MNPs are concentrated only in the treatment area and are irradiated at a low enough frequency to avoid intracellular ion interactions with the electromagnetic field, avoiding raising the temperature in surrounding tissue areas and damaging healthy tissue.

To achieve an effective magnetic fluid-based hyperthermia treatment, continuous research is required on (i) magnetic particle synthesis, (ii) heat dissipation of MNPs, and (iii) heat diffusion, to know the necessary concentration of MNPs for obtaining a temperature greater than 43 °C in the treatment area while the surrounding tissue regulates the temperature.

There are four methods for placing MNPs in cancerous tissue in hyperthermia treatment:

- **Arterial injection:** a magnetic fluid is injected into the arterial stream of the cancerous tissue as the route of administration (Figure 6) [101].
- **Direct injection:** a magnetic fluid is injected directly into the cancerous tissue, with the NPs localizing mainly in the interstitial space. Thus, heat is mainly generated outside the cells when the magnetic pulses are applied. In addition, direct injection of functionalized MNPs with cancer-specific antibodies can be applied [102], decreasing uptake by normal cells (differential endocytosis) and increasing retention of MNPs in cancer tissue.
- **In situ implant formation:** this strategy uses in situ gelation systems, which are injected forming gels directly in the cancerous tissue, trapping the MNPs and consequently improving the focal concentration [103].
- **Active targeting:** the method consists of the surface functionalization of the MNPs with specific antibodies against cancer cells [95], which are injected into the bloodstream, and subsequently accumulated in the desired area through the attraction exerted by an external magnetic field, where the functionalized MNPs end up bind-

ing to cancer cells through cancer-cell-specific receptors and antibodies present on MNPs. However, despite these efforts in the active targeting of MNPs with antibodies, excellent results have not been achieved to date in the accumulation of MNPs in the damaged area, preventing successful hyperthermic treatment.
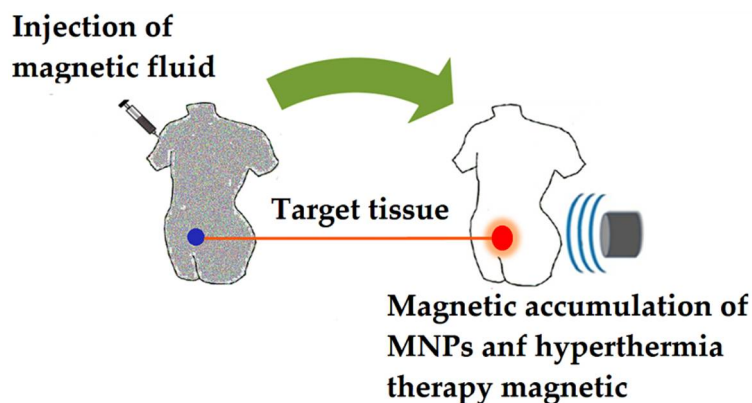

Figure 6. Scheme of therapeutic strategy using MNPs. Functionalized MNPs accumulate in the tumor tissue, then start with the hyperthermia treatment.

5. MNPs in MRI

Nuclear magnetic resonance is mainly applied in the medical field to obtain anatomical and physiological MRI of organs, tissues, bones, and various other internal structures of the body. MRI techniques focus on magnetic field gradients generated by superconducting magnets, making them suitable to replace other diagnostic techniques, including positron emission tomography, myelography, computed tomography, angiography, and subtraction digital radiography, among others. MRI can be used as a tool to examine the soft tissues of the kidney, brain, and liver, as well as for high-magnetic-field evaluations such as chemical biopsy, and can be used preventively due to its ability to detect the magnetic field of paramagnetic deoxyhemoglobin, thereby measuring blood flow to detect future events such as stroke. However, the sensitivity of magnetic resonance devices is reduced when molecular and cellular imaging is used [104].

Generally, to obtain a magnetic scan on a scale of 100 μm through targeted biomarkers, a device equipped with superconducting magnets generates a strong magnetic field T and frequencies below 500 MHz. HTS has been used to fabricate radiofrequency receiving coils used in experimental MRI. However, HTS has several disadvantages due to cryogenic systems and the higher expenses required. Among other shortcomings, HTS materials lack manipulability due to their geometry and length, as well as a suboptimal operation. Consequently, more research is needed to create a feasible HTS MRI to replace standard materials.

In this sense, to improve magnetic resonance by taking maximum advantage of HTS, magnetic compounds capable of improving the quality, contrast, and amplification of the signal have been investigated. Clinically approved compounds include Gd^{3+} and Mn^{2+} compounds due to their strong effect on T1 shortening (longitudinal relaxation), relatively low contrast effects, and minimal retention time in vivo. However, toxicity and biocompatibility have not yet been adequately studied [105]. However, MNPs are more effective as MRI contrast agents because they are better promoters of T2 relaxation (transverse relaxation) than Gd compounds, modifying their magnetic properties by the core size and coating [106].

On the other hand, MNPs have shown their ability as contrast agents to generate soft-tissue images with high resolution and outstanding contrast, showing anatomical details, tissue morphology, and providing therapy against various ailments when loaded or functionalized with therapeutic agents, such as antibodies, peptides, and sugars, among others, providing a possible active targeting towards the affected area. MNPs also stand

out for their null or lack of appreciable toxicity and present longer blood retention times in most cases [107], increasing their capacity for diagnosis and therapy against diseased cells. For example, MNPs functionalized with epithelial growth factors and peptides of the Arg-Gly-Asp type, among others, have been widely proposed as diagnostic agents in different types of cancer [108].

The functionalization of the MNPs not only provides the mentioned advantages but also acts as a coating to improve the operative in vivo; for example, PEG coating is commonly used in iron oxide MNPs [109], which without a coating tend to form aggregates that considerably decrease their magnetic properties in addition to a rapid capture by the cells of the reticular endothelial system.

Some MNPs targeted for MRI were synthesized from Fe_3O_4 cores and subsequently functionalized, thus improving their properties in vivo. For example, Sun et al. synthesized MNPs coated initially with PEG followed by chlorotoxin and Cy5.5 molecules, which are molecules with near-infrared fluorescent properties (Figure 7). MRI and fluorescence microscopy results showed that MNPs could bind effectively to glioma cells, acting as an imaging contrast and as part of diagnosis [110,111]. Similarly, Anbarasu et al. functionalize Fe_3O_4 NPs with monoclonal antibodies, presenting possible active targeting and showing excellent efficacy in MRI [112]. Other MNPs were doped with elements such as Mn and Zn, improving their magnetic properties and increasing the T2 relaxation time, improving MRI contrast [113]. Chee et al. [114] designed iron oxide MNPs functionalized with bisphospholytic peptides, providing high biocompatibility and cell adhesion and showing an improvement in MRI compared with commercial contrast agents.
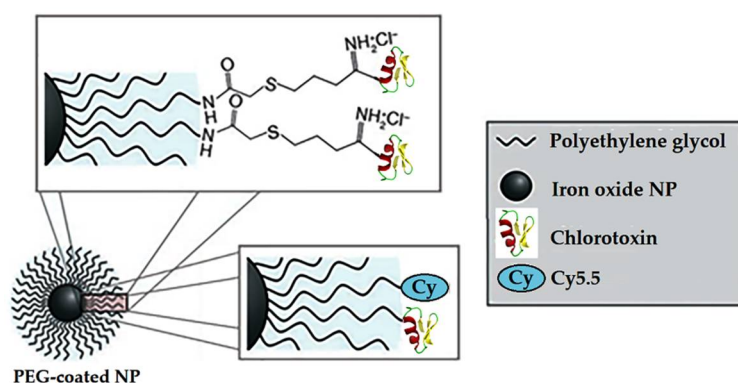

Figure 7. Schematic illustration of MNPs functionalized with clorotoxin and Cy5.5.

6. NPs in Radioterapy Treatment

As previously mentioned, cancer is currently one of the main diseases affecting humanity globally; therefore, the rate of new treatments for this condition has been increasing [115]. Treatments include radiation therapy, which is given to kill cancer cells while sparing healthy tissue. The radiotherapy technique makes use of electron accelerators or beams of ionized particles instead of X-rays, capable of generating powerful radiation energy, which is delivered and directed at cancerous tumors [116,117].

The development of superconducting magnets plays a fundamental role in developing hadronic therapy [118]. Therefore, the application of high-field superconducting cyclotrons represents a critical option for creating compact accelerators with low operating and infrastructure costs since their magnetic design and configuration are equivalent to cyclotrons based on resistive magnets. In addition, other innovations have been made in the design of synchrocyclotrons, showing compact designs without iron in the core, resulting in light coils with a homocentric field capable of generating powerful rays by high acceleration. Furthermore, despite the possible complications of the operation, these synchrocyclotrons and cyclotrons can include various types of ions in a controlled manner that can be applied in appropriate treatments for the patient [119].

Conventional radiotherapy treatments emit beams capable of penetrating tissues, allowing for their application in treating tumors located deep in the body. However, the main complication is the lack of selectivity between tumor cells and healthy cells, limiting the application of these treatments. Future challenges for the development of radiotherapies include targeting radiation doses only to cancerous tissue while enhancing beneficial biological properties. Nanotechnology has provided a crucial advance in cancer treatment. The addition of NPs of elements with high atomic numbers (Z), for example, Pt (Z = 78) and Au (Z = 79), has been shown to reduce radiation damage to healthy tissues in vitro and in vivo [120,121] and increase the yield of free radicals in the area. The probable mechanisms could be explained by a photoelectric effect, releasing X-rays, and short-range Auger-type electron beams, which have an energy lower than 5 keV, energy sufficient to damage DNA and ionize water molecules in medium (Figure 8) [122] and thus expanding the interactions with lower-energy photons at higher atomic numbers [123,124]. The combination of radiotherapy-NPs is an innovative proposal to improve selectivity towards cancer tissue and treatment procedures through an adequate coating of NPs, increasing their circulation time and active direction.
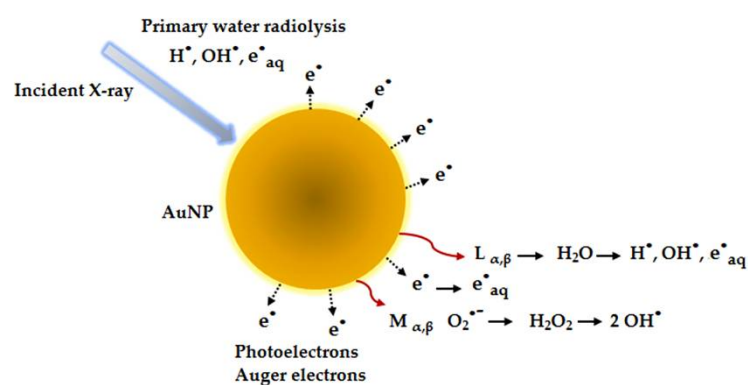

Figure 8. Schematic depiction of increased generation of reactive species by the emission of photo-electrons and Auger electrons from AuNPs in the presence of ionizing radiation.

7. MNPs in Magnetoencephalography (MEG)

Magnetoencephalography (MEG) is a fundamental noninvasive imaging procedure in clinical neuroscience research. It allows for detailed brain-activity mapping by recording high magnetic fields caused by electrical-neuronal currents [125]. MEG operates via high-Tc superconducting quantum interference devices (SQUID), which use liquid nitrogen instead of liquid helium for cooling. MEG can track magnetic brain waves to identify cognitive degeneration such as Alzheimer's disease or seizures [126]. The clear advantage of MEG technology compared to an electroencephalogram and functional MRI is that MEG includes identifying temporal features of brain activation within a thousandth of a second.

The use of MNPs has been reported to improve the efficiency and accuracy of MEG analysis, as SQUID sensors can detect magnetic fields generated by these moving or premagnetized particles [127]. In addition, the results obtained from the investigation helped obtain MEG-type topological maps, which indicate a spatial correlation between the sample's location and the sensor's response. Therefore, these results open the possibility of using MEG to place MNPs inside living organisms.

8. Conclusions

MNPs, in combination with superconducting magnets, have begun to play an essential role in advances in areas such as MDDS, MRI, and hyperthermia, among other fields. Therefore, it is crucial to continue the synthesis of MNPs and developing new superconducting magnets, especially HTS, to better differentiate between the affected and healthy tissue, which is crucial to reaching an optimal complementary therapy.

References

1. Högemann, D.; Ntziachristos, V.; Josephson, L.; Weissleder, R. High throughput magnetic resonance imaging for evaluating targeted nanoparticle probes. *Bioconjug. Chem.* **2002**, *13*, 116–121. [CrossRef]
2. Fortin, J.P.; Gazeau, F.; Wilhelm, C. Intracellular heating of living cells through Néel relaxation of magnetic nanoparticles. *Eur. Biophys. J.* **2008**, *37*, 223–228. [CrossRef] [PubMed]
3. Billotey, C.; Wilhelm, C.; Devaud, M.; Bacri, J.C.; Bittoun, J.; Gazeau, F. Cell internalization of anionic maghemite nanoparticles: Quantitative effect on magnetic resonance imaging. *Magn. Reson. Med.* **2003**, *49*, 646–654. [CrossRef] [PubMed]
4. Moroz, P.; Jones, S.K.; Gray, B.N. Magnetically mediated hyperthermia: Current status and future directions. *Int. J. Hyperth.* **2002**, *18*, 267–284. [CrossRef] [PubMed]
5. Dürr, S.; Janko, C.; Lyer, S.; Tripal, P.; Schwarz, M.; Zaloga, J.; Tietze, R.; Alexiou, C. Magnetic nanoparticles for cancer therapy. *Nanotechnol. Rev.* **2013**, *2*, 395–409. [CrossRef]
6. Sun, C.; Lee, J.S.H.; Zhang, M. Magnetic nanoparticles in MR imaging and drug delivery. *Adv. Drug Deliv. Rev.* **2008**, *60*, 1252–1265. [CrossRef]
7. Chin, A.B.; Yaacob, I.I. Synthesis and characterization of magnetic iron oxide nanoparticles via w/o microemulsion and Massart's procedure. *J. Mater. Process. Technol.* **2007**, *191*, 235–237. [CrossRef]
8. Wan, J.; Chen, X.; Wang, Z.; Yang, X.; Qian, Y. A soft-template-assisted hydrothermal approach to single-crystal Fe_3O_4 nanorods. *J. Cryst. Growth* **2005**, *276*, 571–576. [CrossRef]
9. Kimata, M.; Nakagawa, D.; Hasegawa, M. Preparation of monodisperse magnetic particles by hydrolysis of iron alkoxide. *Powder Technol.* **2003**, *132*, 112–118. [CrossRef]
10. Suslick, K.S.; Fang, M.; Hyeon, T. Sonochemical synthesis of iron colloids. *J. Am. Chem. Soc.* **1996**, *118*, 11960–11961. [CrossRef]
11. Unni, M.; Uhl, A.M.; Savliwala, S.; Savitzky, B.H.; Dhavalikar, R.; Garraud, N.; Arnold, D.P.; Kourkoutis, L.F.; Andrew, J.S.; Rinaldi, C. Thermal decomposition synthesis of iron oxide nanoparticles with diminished magnetic dead layer by controlled addition of oxygen. *ACS Nano* **2017**, *11*, 2284–2303. [CrossRef]
12. Jouyandeh, M.; Zarrintaj, P.; Ganjali, M.R.; Ali, J.A.; Karimzadeh, I.; Aghazadeh, M.; Ghaffari, M.; Saeb, M.R. Curing epoxy with electrochemically synthesized GdxFe3-xO4 magnetic nanoparticles. *Prog. Org. Coat.* **2019**, *136*, 105245. [CrossRef]
13. Salazar-Alvarez, G.; Muhammed, M.; Zagorodni, A.A. Novel flow injection synthesis of iron oxide nanoparticles with narrow size distribution. *Chem. Eng. Sci.* **2006**, *61*, 4625–4633. [CrossRef]
14. López-Saucedo, F.; Flores-Rojas, G.G.; Meléndez-Ortiz, H.I.; Morfín-Gutierrez, A.; Luna-Straffon, M.A.; Bucio, E. Stimuli-responsive nanomaterials for drug delivery. In *Characterization and Biology of Nanomaterials for Drug Delivery. Nanoscience and Nanotechnology in Drug Delivery*; Mohapatra, S.S., Ranjan, S., Dasgupta, N., Mishra, R.K., Thomas, S., Eds.; Elsevier: Amsterdam, The Netherlands, 2019; pp. 375–424.
15. Basak, S.; Chen, D.R.; Biswas, P. Electrospray of ionic precursor solutions to synthesize iron oxide nanoparticles: Modified scaling law. *Chem. Eng. Sci.* **2007**, *62*, 1263–1268. [CrossRef]
16. Andrade, Â.L.; Valente, M.A.; Ferreira, J.M.F.; Fabris, J.D. Preparation of size-controlled nanoparticles of magnetite. *J. Magn. Magn. Mater.* **2012**, *324*, 1753–1757. [CrossRef]
17. Naous, M.; García-Gómez, D.; López-Jiménez, F.J.; Bouanani, F.; Lunar, M.L.; Rubio, S. Multicore magnetic nanoparticles coated with oligomeric micelles: Characterization and potential for the extraction of contaminants over a wide polarity range. *Anal. Chem.* **2017**, *89*, 1353–1361. [CrossRef]
18. Flores-Rojas, G.G.; López-Saucedo, F.; Bucio, E. Gamma-irradiation applied in the synthesis of metallic and organic nanoparticles: A short review. *Radiat. Phys. Chem.* **2020**, *169*, 107962. [CrossRef]

19. Duong, G.V.; Turtelli, R.S.; Nunes, W.C.; Schafler, E.; Hanh, N.; Grössinger, R.; Knobel, M. Ultrafine Co1-xZnxFe2O4 particles synthesized by hydrolysis: Effect of thermal treatment and its relationship with magnetic properties. *J. Non. Cryst. Solids* **2007**, *353*, 805–807. [CrossRef]

20. Rossi, L.M.; Silva, F.P.; Vono, L.L.R.; Kiyohara, P.K.; Duarte, E.L.; Itri, R.; Landers, R.; Machado, G. Superparamagnetic nanoparticle-supported palladium: A highly stable magnetically recoverable and reusable catalyst for hydrogenation reactions. *Green Chem.* **2007**, *9*, 379. [CrossRef]

21. Kumar, A.; Rana, P.S.; Yadav, M.S.; Pant, R.P. Effect of Gd^{3+} ion distribution on structural and magnetic properties in nano-sized Mn–Zn ferrite particles. *Ceram. Int.* **2015**, *41*, 1297–1302. [CrossRef]

22. De Silva, C.R.; Smith, S.; Shim, I.; Pyun, J.; Gutu, T.; Jiao, J.; Zheng, Z. Lanthanide(III)-doped magnetite nanoparticles. *J. Am. Chem. Soc.* **2009**, *131*, 6336–6337. [CrossRef] [PubMed]

23. Ebisawa, Y.; Miyaji, F.; Kokubo, T.; Ohura, K.; Nakamura, T. Bioactivity of ferrimagnetic glass-ceramics in the system FeO-Fe2O3-CaO-SiO2. *Biomaterials* **1997**, *18*, 1277–1284. [CrossRef]

24. Hariani, P.L.; Faizal, M.; Setiabudidaya, D. Synthesis and properties of Fe3O4 nanoparticles by Co-precipitation method to removal procion dye. *Int. J. Environ. Sci. Dev.* **2013**, *4*, 336–340. [CrossRef]

25. Samad, A.; Beg, S.; Nazish, I. *Liposomal Delivery Systems: Advances and Challenges*; Samad, A., Beg, S., Nazish, I., Eds.; Future Science Ltd.: London, UK; Panacea Biotec Ltd.: New Delhi, India, 2015; Volume 1, ISBN 978-1-910419-05-2.

26. Sivakumar, M.; Kanagesan, S.; Chinnaraj, K.; Suresh Babu, R.; Nithiyanantham, S. Synthesis, characterization and effects of citric acid and PVA on magnetic properties of CoFe2O4. *J. Inorg. Organomet. Polym. Mater.* **2013**, *23*, 439–445. [CrossRef]

27. Park, J.; An, K.; Hwang, Y.; Park, J.E.G.; Noh, H.J.; Kim, J.Y.; Park, J.H.; Hwang, N.M.; Hyeon, T. Ultra-large-scale syntheses of monodisperse nanocrystals. *Nat. Mater.* **2004**, *3*, 891–895. [CrossRef] [PubMed]

28. Jeraal, M.I.; Roberts, K.J.; McRobbie, I.; Harbottle, D. Assessment of the thermal degradation of sodium lauroyl isethionate using predictive isoconversional kinetics and a temperature-resolved analysis of evolved gases. *Ind. Eng. Chem. Res.* **2019**, *58*, 8112–8122. [CrossRef]

29. Stojanovic, B.; Dzunuzovic, A.; Ilic, N. Review of methods for the preparation of magnetic metal oxides. In *Magnetic, Ferroelectric, and Multiferroic Metal Oxides*; Stojanovic, B., Ed.; Elsevier: Amsterdam, The Netherlands, 2018; pp. 333–359.

30. Sun, S.; Zeng, H.; Robinson, D.B.; Raoux, S.; Rice, P.M.; Wang, S.X.; Li, G. Monodisperse MFe2O4 (M=Fe, Co, Mn) nanoparticles. *J. Am. Chem. Soc.* **2004**, *126*, 273–279. [CrossRef]

31. Sun, S.; Zeng, H. Size-controlled synthesis of magnetite nanoparticles. *J. Am. Chem. Soc.* **2002**, *124*, 8204–8205. [CrossRef]

32. Shevchenko, E.V.; Talapin, D.V.; Rogach, A.L.; Kornowski, A.; Haase, M.; Weller, H. Colloidal synthesis and self-assembly of CoPt3 nanocrystals. *J. Am. Chem. Soc.* **2002**, *124*, 11480–11485. [CrossRef]

33. Sun, S.; Murray, C.B.; Weller, D.; Folks, L.; Moser, A. Monodisperse FePt nanoparticles and ferromagnetic FePt nanocrystal superlattices. *Science* **2000**, *287*, 1989–1992. [CrossRef]

34. Yamada, Y.; Suzuki, T.; Abarra, E.N. Magnetic properties of electron beam evaporated CoPt alloy thin films. *IEEE Trans. Magn.* **1998**, *34*, 343–345. [CrossRef]

35. Jana, N.R.; Chen, Y.; Peng, X. Size- and shape-controlled magnetic (Cr, Mn, Fe, Co, Ni) oxide nanocrystals via a simple and general approach. *Chem. Mater.* **2004**, *16*, 3931–3935. [CrossRef]

36. Li, Z.; Sun, Q.; Gao, M. Preparation of water-soluble magnetite nanocrystals from hydrated ferric salts in 2-pyrrolidone: Mechanism leading to Fe3O4. *Angew. Chemie Int. Ed.* **2005**, *44*, 123–126. [CrossRef]

37. Hu, F.; Wei, L.; Zhou, Z.; Ran, Y.; Li, Z.; Gao, M. Preparation of biocompatible magnetite nanocrystals for in vivo magnetic resonance detection of cancer. *Adv. Mater.* **2006**, *18*, 2553–2556. [CrossRef]

38. Butter, K.; Philipse, A.P.; Vroege, G.J. Synthesis and properties of iron ferrofluids. *J. Magn. Magn. Mater.* **2002**, *252*, 1–3. [CrossRef]

39. Paul, B.K.; Moulik, S.P. Uses and applications of microemulsions Uses and applications of microemulsions. *Curr. Sci.* **2001**, *80*, 990–1001.

40. Liu, C.; Zou, B.; Rondinone, A.J.; Zhang, Z.J. Reverse micelle synthesis and characterization of superparamagnetic MnFe2O4 spinel ferrite nanocrystallites. *J. Phys. Chem. B* **2000**, *104*, 1143–1145. [CrossRef]

41. Moumen, N.; Pileni, M.P. Control of the size of cobalt ferrite magnetic fluid. *J. Phys. Chem.* **1996**, *100*, 1867–1873. [CrossRef]

42. Poornima Vijayan, P.; Somadas Radhamany, A.; Ereath Beeran, A.; Jouyandeh, M.; Reza Saeb, M. Magnetic nanoparticles-based coatings. In *Nanotechnology in the Automotive Industry*; Song, H., Nguyen, T.A., Yasin, G., Singh, N.B., Gupta, R.K., Eds.; Elsevier: Amsterdam, The Netherlands, 2022; pp. 317–343.

43. Lee, H.; Lee, E.; Kim, D.K.; Jang, N.K.; Jeong, Y.Y.; Jon, S. Antibiofouling polymer-coated superparamagnetic iron oxide nanoparticles as potential magnetic resonance contrast agents for in vivo cancer imaging. *J. Am. Chem. Soc.* **2006**, *128*, 7383–7389. [CrossRef]

44. Berry, C.C.; Wells, S.; Charles, S.; Aitchison, G.; Curtis, A.S.G. Cell response to dextran-derivatised iron oxide nanoparticles post internalisation. *Biomaterials* **2004**, *25*, 5405–5413. [CrossRef]

45. Jodin, L.; Dupuis, A.C.; Rouvière, E.; Reiss, P. Influence of the catalyst type on the growth of carbon nanotubes via methane chemical vapor deposition. *J. Phys. Chem. B* **2006**, *110*, 7328–7333. [CrossRef] [PubMed]

46. Nitin, N.; LaConte, L.E.W.; Zurkiya, O.; Hu, X.; Bao, G. Functionalization and peptide-based delivery of magnetic nanoparticles as an intracellular MRI contrast agent. *JBIC J. Biol. Inorg. Chem.* **2004**, *9*, 706–712. [CrossRef] [PubMed]

47. Lee, H.; Mi, K.Y.; Park, S.; Moon, S.; Jung, J.M.; Yong, Y.J.; Kang, H.W.; Jon, S. Thermally cross-linked superparamagnetic iron oxide nanoparticles: Synthesis and application as a dual imaging probe for cancer in vivo. *J. Am. Chem. Soc.* **2007**, *129*, 12739–12745. [CrossRef] [PubMed]

48. Kumagai, M.; Imai, Y.; Nakamura, T.; Yamasaki, Y.; Sekino, M.; Ueno, S.; Hanaoka, K.; Kikuchi, K.; Nagano, T.; Kaneko, E.; et al. Iron hydroxide nanoparticles coated with poly(ethylene glycol)-poly(aspartic acid) block copolymer as novel magnetic resonance contrast agents for in vivo cancer imaging. *Colloids Surf. B Biointerfaces* **2007**, *56*, 174–181. [CrossRef]

49. LaConte, L.E.W.; Nitin, N.; Zurkiya, O.; Caruntu, D.; O'Connor, C.J.; Hu, X.; Bao, G. Coating thickness of magnetic iron oxide nanoparticles affects R_2 relaxivity. *J. Magn. Reson. Imaging* **2007**, *26*, 1634–1641. [CrossRef]

50. Krishnan, K.M. Biomedical nanomagnetics: A spin through possibilities in imaging, diagnostics, and therapy. *IEEE Trans. Magn.* **2010**, *46*, 2523–2558. [CrossRef]

51. Lartigue, L.; Coupeau, M.; Lesault, M. Luminophore and magnetic multicore nanoassemblies for dual-mode MRI and fluorescence imaging. *Nanomaterials* **2019**, *10*, 28. [CrossRef]

52. Sheng, Y.; Liu, C.; Yuan, Y.; Tao, X.; Yang, F.; Shan, X.; Zhou, H.; Xu, F. Long-circulating polymeric nanoparticles bearing a combinatorial coating of PEG and water-soluble chitosan. *Biomaterials* **2009**, *30*, 2340–2348. [CrossRef]

53. Wang, J.; Zhang, B.; Wang, L.; Wang, M.; Gao, F. One-pot synthesis of water-soluble superparamagnetic iron oxide nanoparticles and their MRI contrast effects in the mouse brains. *Mater. Sci. Eng. C* **2015**, *48*, 416–423. [CrossRef]

54. Wiseman, J.W.; Goddard, C.A.; McLelland, D.; Colledge, W.H. A comparison of linear and branched polyethylenimine (PEI) with DCChol/DOPE liposomes for gene delivery to epithelial cells in vitro and in vivo. *Gene Ther.* **2003**, *10*, 1654–1662. [CrossRef]

55. Zakeri, A.; Kouhbanani, M.A.J.; Beheshtkhoo, N.; Beigi, V.; Mousavi, S.M.; Hashemi, S.A.R.; Karimi Zade, A.; Amani, A.M.; Savardashtaki, A.; Mirzaei, E.; et al. Polyethylenimine-based nanocarriers in co-delivery of drug and gene: A developing horizon. *Nano Rev. Exp.* **2018**, *9*, 1488497. [CrossRef]

56. Vicennati, P.; Giuliano, A.; Ortaggi, G.; Masotti, A. Polyethylenimine in medicinal chemistry. *Curr. Med. Chem.* **2008**, *15*, 2826–2839. [CrossRef]

57. Li, J.; Zhou, Y.; Li, M.; Xia, N.; Huang, Q.; Do, H.; Liu, Y.N.; Zhou, F. Carboxymethylated dextran-coated magnetic iron oxide nanoparticles for regenerable bioseparation. *J. Nanosci. Nanotechnol.* **2011**, *11*, 10187–10192. [CrossRef]

58. Rivera-Hernández, G.; Antunes-Ricardo, M.; Martínez-Morales, P.; Sánchez, M.L. Polyvinyl alcohol based-drug delivery systems for cancer treatment. *Int. J. Pharm.* **2021**, *600*, 120478. [CrossRef]

59. Salunkhe, A.B.; Khot, V.M.; Thorat, N.D.; Phadatare, M.R.; Sathish, C.I.; Dhawale, D.S.; Pawar, S.H. Polyvinyl alcohol functional-ized cobalt ferrite nanoparticles for biomedical applications. *Appl. Surf. Sci.* **2013**, *264*, 598–604. [CrossRef]

60. Vu-Quang, H.; Muthiah, M.; Lee, H.J.; Kim, Y.K.; Rhee, J.H.; Lee, J.H.; Cho, C.S.; Choi, Y.J.; Jeong, Y.Y.; Park, I.K. Immune cell-specific delivery of beta-glucan-coated iron oxide nanoparticles for diagnosing liver metastasis by MR imaging. *Carbohydr. Polym.* **2012**, *87*, 1159–1168. [CrossRef]

61. Patel, A.; Asik, D.; Snyder, E.M.; Dilillo, A.E.; Cullen, P.J.; Morrow, J.R. Binding and release of FeIII complexes from glucan particles for the delivery of T_1 MRI contrast agents. *ChemMedChem* **2020**, *15*, 1050–1057. [CrossRef]

62. Soto, E.R.; Caras, A.C.; Kut, L.C.; Castle, M.K.; Ostroff, G.R. Glucan particles for macrophage argeted delivery of nanoparticles. *J. Drug Deliv.* **2012**, *2012*, 143524. [CrossRef]

63. Hwang, J.; Son, J.; Seo, Y.; Jo, Y.; Lee, K.; Lee, D.; Khan, M.S.; Chavan, S.; Park, C.; Sharma, A.; et al. Functional silica nanoparticles conjugated with beta-glucan to deliver anti-tuberculosis drug molecules. *J. Ind. Eng. Chem.* **2018**, *58*, 376–385. [CrossRef]

64. Su, Y.; Chen, L.; Yang, F.; Cheung, P.C.K. Beta-d-glucan-based drug delivery system and its potential application in targeting tumor associated macrophages. *Carbohydr. Polym.* **2021**, *253*, 117258. [CrossRef]

65. Langereis, S.; Geelen, T.; Grüll, H.; Strijkers, G.J.; Nicolay, K. Paramagnetic liposomes for molecular MRI and MRI-guided drug delivery. *NMR Biomed.* **2013**, *26*, 728–744. [CrossRef]

66. Kamaly, N.; Miller, A.D. Paramagnetic liposome nanoparticles for cellular and tumour imaging. *Int. J. Mol. Sci.* **2010**, *11*, 1759–1776. [CrossRef]

67. Al-Jamal, W.T.; Kostarelos, K. Liposomes: From a clinically established drug delivery system to a nanoparticle platform for theranostic nanomedicine. *Acc. Chem. Res.* **2011**, *44*, 1094–1104. [CrossRef]

68. Mikhaylov, G.; Mikac, U.; Magaeva, A.A.; Itin, V.I.; Naiden, E.P.; Psakhye, I.; Babes, L.; Reinheckel, T.; Peters, C.; Zeiser, R.; et al. Ferri-liposomes as an MRI-visible drug-delivery system for targeting tumours and their microenvironment. *Nat. Nanotechnol.* **2011**, *6*, 594–602. [CrossRef]

69. Wang, J.J.; Zeng, Z.W.; Xiao, R.Z.; Xie, T.; Zhou, G.L.; Zhan, X.R.; Wang, S.L. Recent advances of chitosan nanoparticles as drug carriers. *Int. J. Nanomed.* **2011**, *6*, 765–774. [CrossRef]

70. Song, G.; Cheng, L.; Chao, Y.; Yang, K.; Liu, Z. Emerging nanotechnology and advanced materials for cancer radiation therapy. *Adv. Mater.* **2017**, *29*, 1700996. [CrossRef]

71. Safari, A.; Sarikhani, A.; Shahbazi-Gahrouei, D.; Alamzadeh, Z.; Beik, J.; Dezfuli, A.S.; Mahabadi, V.P.; Tohfeh, M.; Shakeri-Zadeh, A. Optimal scheduling of the nanoparticle-mediated cancer photo-thermo-radiotherapy. *Photodiagn. Photodyn. Ther.* **2020**, *32*, 102061. [CrossRef]

72. Wang, D.; Wang, S.; Zhou, Z.; Bai, D.; Zhang, Q.; Ai, X.; Gao, W.; Zhang, L. White blood cell membrane-coated nanoparticles: Recent development and medical applications. *Adv. Healthc. Mater.* **2022**, *11*, 2101349. [CrossRef]

73. Narain, A.; Asawa, S.; Chhabria, V.; Patil-Sen, Y. Cell membrane coated nanoparticles: Next-generation therapeutics. *Nanomedicine* **2017**, *12*, 2677–2692. [CrossRef] [PubMed]

74. Yoshida, Y.; Fukui, S.; Fujimoto, S.; Mishima, F.; Takeda, S.; Izumi, Y.; Ohtani, S.; Fujitani, Y.; Nishijima, S. Ex Vivo investigation of magnetically targeted drug delivery system. *J. Magn. Magn. Mater.* **2007**, *310*, 2880–2882. [CrossRef]

75. Mishima, F.; Takeda, S.I.; Izumi, Y.; Nishijima, S. Three dimensional motion control system of ferromagnetic particles for magnetically targeted drug delivery systems. *IEEE Trans. Appl. Supercond.* **2006**, *16*, 1539–1542. [CrossRef]

76. Alexiou, C.; Schmid, R.J.; Jurgons, R.; Kremer, M.; Wanner, G.; Bergemann, C.; Huenges, E.; Nawroth, T.; Arnold, W.; Parak, F.G. Targeting cancer cells: Magnetic nanoparticles as drug carriers. *Eur. Biophys. J.* **2006**, *35*, 446–450. [CrossRef] [PubMed]

77. Morishita, N.; Nakagami, H.; Morishita, R.; Takeda, S.I.; Mishima, F.; Terazono, B.; Nishijima, S.; Kaneda, Y.; Tanaka, N. Magnetic nanoparticles with surface modification enhanced gene delivery of HVJ-E vector. *Biochem. Biophys. Res. Commun.* **2005**, *334*, 1121–1126. [CrossRef] [PubMed]

78. Bednorz, J.G.; Takashige, M.; Müller, K.A. Susceptibility measurements support high-Tcsuperconductivity in the Ba-La-Cu-O system. *Prop. Perovskites Other Oxides* **2010**, *193*, 555–565. [CrossRef]

79. Baker, I. Magnetic nanoparticle synthesis. In *Nanobiomaterials*; Narayan, R., Ed.; Elsevier: Amsterdam, The Netherlands, 2018; pp. 197–229. ISBN 9780081007167.

80. Barnsley, L.C.; Carugo, D.; Owen, J.; Stride, E. Halbach arrays consisting of cubic elements optimised for high field gradients in magnetic drug targeting applications. *Phys. Med. Biol.* **2015**, *60*, 8303–8327. [CrossRef]

81. Owen, J.; Rademeyer, P.; Chung, D.; Cheng, Q.; Holroyd, D.; Coussios, C.; Friend, P.; Pankhurst, Q.A.; Stride, E. Magnetic targeting of microbubbles against physiologically relevant flow conditions. *Interface Focus* **2015**, *5*, 20150001. [CrossRef]

82. Nishijima, S.; Takeda, S.I.; Mishima, F.; Tabata, Y.; Yamamoto, M.; Joh, J.I.; Iseki, H.; Muragaki, Y.; Sasaki, A.; Kubota, J.; et al. A study of magnetic drug delivery system using bulk high temperature superconducting magnet. *IEEE Trans. Appl. Supercond.* **2008**, *18*, 874–877. [CrossRef]

83. Nakagawa, K.; Mishima, F.; Akiyama, Y.; Nishijima, S. Study on magnetic drug delivery system using HTS bulk magnet. *IEEE Trans. Appl. Supercond.* **2012**, *22*, 4–7. [CrossRef]

84. Kamihara, Y.; Watanabe, T.; Hirano, M.; Hosono, H. Iron-based layered superconductor La $[O_{1-x} F_x]$ FeAs (x = 0.05–0.12) with T_c = 26 K. *J. Am. Chem. Soc.* **2008**, *130*, 3296–3297. [CrossRef]

85. Pankhurst, Q.A.; Thanh, N.K.T.; Jones, S.K.; Dobson, J. Progress in applications of magnetic nanoparticles in biomedicine. *J. Phys. D. Appl. Phys.* **2009**, *42*, 224001. [CrossRef]

86. Nariki, S.; Sakai, N.; Murakami, M. Melt-processed Gd-Ba-Cu-O superconductor with trapped field of 3 T at 77 K. *Supercond. Sci. Technol.* **2005**, *18*, S126. [CrossRef]

87. Ganin, A.Y.; Takabayashi, Y.; Khimyak, Y.Z.; Margadonna, S.; Tamai, A.; Rosseinsky, M.J.; Prassides, K. Bulk superconductivity at 38 K in a molecular system. *Nat. Mater.* **2008**, *7*, 367–371. [CrossRef]

88. Dietmar Drung High-T_c and low-T_c dc SQUID electronics. *Supercond. Sci. Technol.* **2003**, *16*, 1320. [CrossRef]

89. Huang, H.S.; Hainfeld, J.F. IJN-43770-intravenous-magnetic-nanoparticle-hyperthermia. *Int. J. Nanomed.* **2013**, *8*, 2521–2532.

90. Foster, K.R. Thermal and nonthermal mechanisms of interaction of radio-frequency energy with biological systems. *IEEE Trans. Plasma Sci.* **2000**, *28*, 15–23. [CrossRef]

91. Wang, X.; Qin, J.; Zhang, Y.; Ma, J. Stimuli-responsive self-regulating magnetic-thermal materials for selective magnetic hyperthermia therapy. *OpenNano* **2022**, *7*, 100052. [CrossRef]

92. Jordan, A.; Wust, P.; Fähling, H.; John, W.; Hinz, A.; Felix, R. Inductive heating of ferrimagnetic particles and magnetic fluids: Physical evaluation of their potential for hyperthermia. *Int. J. Hyperth.* **2009**, *25*, 499–511. [CrossRef]

93. Mortezaee, K.; Narmani, A.; Salehi, M.; Bagheri, H.; Farhood, B.; Haghi-Aminjan, H.; Najafi, M. Synergic effects of nanoparticles-mediated hyperthermia in radiotherapy/chemotherapy of cancer. *Life Sci.* **2021**, *269*, 119020. [CrossRef]

94. Mahmoudi, M.; Sant, S.; Wang, B.; Laurent, S.; Sen, T. Superparamagnetic iron oxide nanoparticles (SPIONs): Development, surface modification and applications in chemotherapy. *Adv. Drug Deliv. Rev.* **2011**, *63*, 24–46. [CrossRef]

95. Ito, A.; Shinkai, M.; Honda, H.; Kobayashi, T. Medical application of functionalized magnetic nanoparticles. *J. Biosci. Bioeng.* **2005**, *100*, 1–11. [CrossRef]

96. Nandhini, G.; Shobana, M.K. Role of ferrite nanoparticles in hyperthermia applications. *J. Magn. Magn. Mater.* **2022**, *552*, 169236. [CrossRef]

97. Laurent, S.; Forge, D.; Port, M.; Roch, A.; Robic, C.; Vander Elst, L.; Muller, R.N. Magnetic iron oxide nanoparticles: Synthesis, stabilization, vectorization, physicochemical characterizations, and biological applications. *Chem. Rev.* **2008**, *108*, 2064–2110. [CrossRef]

98. Rosensweig, R.E. Heating magnetic fluid with alternating magnetic field. *J. Magn. Magn. Mater.* **2002**, *252*, 370–374. [CrossRef]

99. Maier-Hauff, K.; Rothe, R.; Scholz, R.; Gnveckow, U.; Wust, P.; Thiesen, B.; Feussner, A.; Deimling, A.; Waldoefner, N.; Felix, R.; et al. Intracranial thermotherapy using magnetic nanoparticles combined with external beam radiotherapy: Results of a feasibility study on patients with glioblastoma multiforme. *J. Neurooncol.* **2007**, *81*, 53–60. [CrossRef]

100. Van den Berg, C.A.T.; Bartels, L.W.; De Leeuw, A.A.C.; Lagendijk, J.J.W.; Van de Kamer, J.B. Experimental validation of hyperthermia SAR treatment planning using MR B^{1+} imaging. *Phys. Med. Biol.* **2004**, *49*, 5029–5042. [CrossRef]

101. Tang, Y.-D.; Zou, J.; Flesch, R.C.C.; Jin, T. Effect of injection strategy for nanofluid transport on thermal damage behavior inside biological tissue during magnetic hyperthermia. *Int. Commun. Heat Mass Transf.* **2022**, *133*, 105979. [CrossRef]

102. Peng, X.H.; Qian, X.; Mao, H.; Wang, A.Y.; Chen, Z.G.; Nie, S.; Shin, D.M. Targeted magnetic iron oxide nanoparticles for tumor imaging and therapy. *Int. J. Nanomed.* **2008**, *3*, 311–321. [CrossRef]

103. Le Renard, P.E.; Jordan, O.; Faes, A.; Petri-Fink, A.; Hofmann, H.; Rüfenacht, D.; Bosman, F.; Buchegger, F.; Doelker, E. The in vivo performance of magnetic particle-loaded injectable, in situ gelling, carriers for the delivery of local hyperthermia. *Biomaterials* **2010**, *31*, 691–705. [CrossRef] [PubMed]

104. Bradbury, M.; Hricak, H. Molecular MR imaging in oncology. *Magn. Reson. Imaging Clin. N. Am.* **2005**, *13*, 225–240. [CrossRef] [PubMed]

105. Bulte, J.W.M.; Kraitchman, D.L. Iron oxide MR contrast agents for molecular and cellular imaging. *NMR Biomed.* **2004**, *17*, 484–499. [CrossRef] [PubMed]

106. Rogers, W.J.; Basu, P. Factors regulating macrophage endocytosis of nanoparticles: Implications for targeted magnetic resonance plaque imaging. *Atherosclerosis* **2005**, *178*, 67–73. [CrossRef]

107. Montet, X.; Montet-Abou, K.; Reynolds, F.; Weissleder, R.; Josephson, L. Nanoparticle imaging of integrins on tumor cells. *Neoplasia* **2006**, *8*, 214–222. [CrossRef]

108. Ng, Q.K.T.; Su, H.; Armijo, A.L.; Czernin, J.; Radu, C.G.; Segura, T. Clustered Arg-Gly-Asp peptides enhances tumor targeting of nonviral vectors. *ChemMedChem* **2011**, *6*, 623–627. [CrossRef]

109. Lazaro-Carrillo, A.; Filice, M.; Guillén, M.J.; Amaro, R.; Viñambres, M.; Tabero, A.; Paredes, K.O.; Villanueva, A.; Calvo, P.; del Puerto Morales, M.; et al. Tailor-made PEG coated iron oxide nanoparticles as contrast agents for long lasting magnetic resonance molecular imaging of solid cancers. *Mater. Sci. Eng. C* **2020**, *107*, 110262. [CrossRef]

110. Sun, C.; Veiseh, O.; Gunn, J.; Fang, C.; Hansen, S.; Lee, D.; Sze, R.; Ellenbogen, R.G.; Olson, J.; Zhang, M. In Vivo MRI detection of gliomas by chlorotoxin-conjugated superparamagnetic nanoprobes. *Small* **2008**, *4*, 372–379. [CrossRef]

111. Veiseh, O.; Sun, C.; Gunn, J.; Kohler, N.; Gabikian, P.; Lee, D.; Bhattarai, N.; Ellenbogen, R.; Sze, R.; Hallahan, A.; et al. Optical and MRI multifunctional nanoprobe for targeting gliomas. *Nano Lett.* **2005**, *5*, 1003–1008. [CrossRef]

112. Anbarasu, M.; Anandan, M.; Chinnasamy, E.; Gopinath, V.; Balamurugan, K. Synthesis and characterization of polyethylene glycol (PEG) coated Fe_3O_4 nanoparticles by chemical co-precipitation method for biomedical applications. *Spectrochim. Acta-Part A Mol. Biomol. Spectrosc.* **2015**, *135*, 536–539. [CrossRef]

113. Chen, H.J.; Zhang, Z.H.; Luo, L.J.; Yao, S.Z. Surface-imprinted chitosan-coated magnetic nanoparticles modified multi-walled carbon nanotubes biosensor for detection of bovine serum albumin. *Sens. Actuators B Chem.* **2012**, *163*, 76–83. [CrossRef]

114. Chee, H.L.; Gan, C.R.R.; Ng, M.; Low, L.; Fernig, D.G.; Bhakoo, K.K.; Paramelle, D. Biocompatible peptide-coated ultrasmall superparamagnetic iron oxide nanoparticles for in vivo contrast-enhanced magnetic resonance imaging. *ACS Nano* **2018**, *12*, 6480–6491. [CrossRef]

115. Geng, H.; Zhou, M.; Li, B.; Liu, L.; Yang, X.; Wen, Y.; Yu, H.; Wang, H.; Chen, J.; Chen, L. Metal-drug nanoparticles-mediated osteolytic microenvironment regulation for enhanced radiotherapy of orthotopic osteosarcoma. *Chem. Eng. J.* **2021**, *417*, 128103. [CrossRef]

116. Durante, M.; Loeffler, J.S. Charged particles in radiation oncology. *Nat. Rev. Clin. Oncol.* **2010**, *7*, 37–43. [CrossRef] [PubMed]

117. Schüller, A.; Heinrich, S.; Fouillade, C.; Subiel, A.; De Marzi, L.; Romano, F.; Peier, P.; Trachsel, M.; Fleta, C.; Kranzer, R.; et al. The european joint research project UHDpulse—Metrology for advanced radiotherapy using particle beams with ultra-high pulse dose rates. *Phys. Medica* **2020**, *80*, 134–150. [CrossRef] [PubMed]

118. Brero, F.; Albino, M.; Antoccia, A.; Arosio, P.; Avolio, M.; Berardinelli, F.; Bettega, D.; Calzolari, P.; Ciocca, M.; Corti, M.; et al. Hadron therapy, magnetic nanoparticles and hyperthermia: A promising combined tool for pancreatic cancer treatment. *Nanomaterials* **2020**, *10*, 1919. [CrossRef] [PubMed]

119. Wang, X.; Smirnov, V.; Vorozhtsov, S. Superconducting cyclotron for flash therapy. *Nucl. Instrum. Methods Phys. Res. Sect. A Accel. Spectrometers Detect. Assoc. Equip.* **2021**, *986*, 164742. [CrossRef]

120. Cooper, D.R.; Bekah, D.; Nadeau, J.L. Gold nanoparticles and their alternatives for radiation therapy enhancement. *Front. Chem.* **2014**, *2*, 86. [CrossRef]

121. Li, W.; Li, X.; Liu, S.; Yang, W.; Pan, F.; Yang, X.Y.; Du, B.; Qin, L.; Pan, Y. Gold nanoparticles attenuate metastasis by tumor vasculature normalization and epithelial-mesenchymal transition inhibition. *Int. J. Nanomed.* **2017**, *12*, 3509–3520. [CrossRef]

122. Schuemann, J.; Berbeco, R.; Chithrani, D.B.; Cho, S.H.; Kumar, R.; McMahon, S.J.; Sridhar, S.; Krishnan, S. Roadmap to clinical use of gold nanoparticles for radiation sensitization. *Int. J. Radiat. Oncol. Biol. Phys.* **2016**, *94*, 189–205. [CrossRef]

123. Detappe, A.; Kunjachan, S.; Rottmann, J.; Robar, J.; Tsiamas, P.; Korideck, H.; Tillement, O.; Berbeco, R. AGuIX nanoparticles as a promising platform for image-guided radiation therapy. *Cancer Nanotechnol.* **2015**, *6*, 4. [CrossRef]

124. Popovtzer, A.; Mizrachi, A.; Motiei, M.; Bragilovski, D.; Lubimov, L.; Levi, M.; Hilly, O.; Ben-Aharon, I.; Popovtzer, R. Actively targeted gold nanoparticles as novel radiosensitizer agents: An in vivo head and neck cancer model. *Nanoscale* **2016**, *8*, 2678–2685. [CrossRef]

125. Schneiderman, J.F. Information content with low- vs. high-Tc SQUID arrays in MEG recordings: The case for high-Tc SQUID-based MEG. *J. Neurosci. Methods* **2014**, *222*, 42–46. [CrossRef]

126. Maestú, F.; Cuesta, P.; Hasan, O.; Fernández, A.; Funke, M.; Schulz, P.E. The importance of the validation of M/EEG with current biomarkers in Alzheimer's disease. *Front. Hum. Neurosci.* **2019**, *13*, 17. [CrossRef]

127. Andersen, L.M.; Pfeiffer, C.; Ruffieux, S.; Riaz, B.; Winkler, D.; Schneiderman, J.F.; Lundqvist, D. On-scalp MEG SQUIDs are sensitive to early somatosensory activity unseen by conventional MEG. *Neuroimage* **2020**, *221*, 117157. [CrossRef]